Supporting Information

Steering Lu_3N cluster in $C_{76\text{-}78}$ cages：Cluster configuration dominated by cage transformation

Pengwei Yu, Shuaifeng Hu, Xinyue Tian, Wangqiang Shen, Pengyuan Yu, Kun Guo Yunpeng Xie, Lipiao Bao* and Xing Lu*

State Key Laboratory of Materials Processing and Die & Mould Technology, School of Materials Science and Engineering, Huazhong University of Science and Technology, 1037 Luoyu Road, Wuhan, 430074 China. E-mail: baol@hust.edu.cn; lux@hust.edu.cn

Table of Contents

High-performance Liquid Chromatography (HPLC) Separation Processes of $Lu_3N@C_{76, 78}$. $Lu_3N@C_{76, 78}$ isomers were isolated by a multiple-stage HPLC process using toluene as the eluent. The first stage was performed on a Buckyprep column (20 mm × 250 mm, Cosmosil Nacalai Tesque), and three fractions named as Fr5, Fr6 and Fr8 were collected (Fig. S1). Then, Fr6 was injected into a Buckyprep column (20 mm × 250 mm, Cosmosil Nacalai Tesque) for the second stage separation, and a truncated fraction named as Fr6-4 was collected to increase the proportion of $Lu_3N@C_s(17490)$-C_{76} (Fig. S2a). Fr6-4 was then injected into a 5PBB column (20 mm × 250 mm, Cosmosil Nacalai Tesque), and $Lu_3N@C_s(17490)$-C_{76} was finally obtained (Fig. S2b).

In the second stage for the purification of $Lu_3N@C_2(22010)$-C_{78}, a Buckyprep-M column (20 mm × 250 mm, Cosmosil Nacalai Tesque) was used to separate Fr8, then a fraction named as Fr8-2 was collected (Fig. S3a). Fr8-2 was injected into a Buckyprep-M column (20 mm × 250 mm, Cosmosil Nacalai Tesque), and a fraction named as Fr8-2-2 was collected (Fig. S3b). In the last, Fr8-2-2 was injected into a Buckyprep column (20 mm × 250 mm, Cosmosil Nacalai Tesque), and pure $Lu_3N@C_2(22010)$-C_{78} was finally obtained (Fig. S3c).

Moreover, Fr5 was injected into a Buckyprep-M column (20 mm × 250 mm, Cosmosil Nacalai Tesque), a fraction named as Fr5-3 was obtained (Figure S4a). In the third stage, fraction Fr5-3 was injected into a Buckyprep column (20 mm × 250 mm, Cosmosil Nacalai Tesque), and a truncated fraction Fr5-3-3 was collected to increase the proportion of $Lu_3N@D_{3h}(5)$-C_{78} (Fig. S4b). After that, Fr5-3-3-3 was injected into a Buckyprep column (10 mm × 250 mm, Cosmosil Nacalai Tesque), and pure $Lu_3N@D_{3h}(5)$-C_{78} was obtained (Fig. S4c).

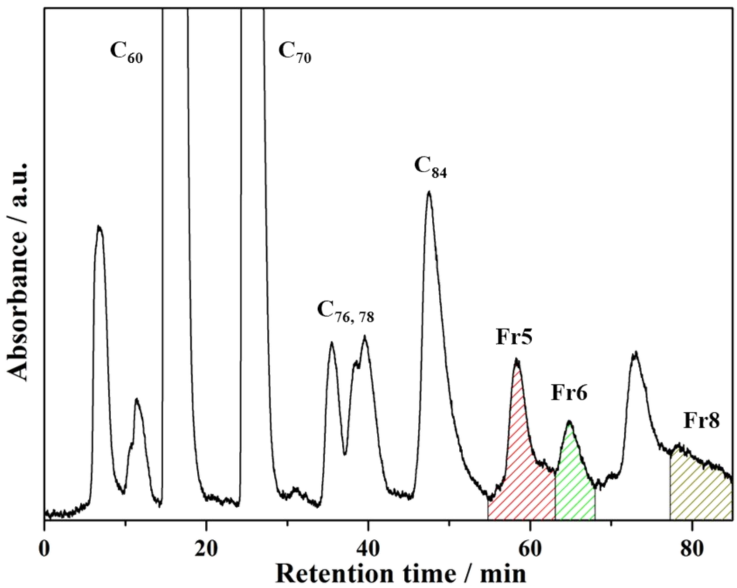

Fig. S1 Isolation scheme of the fullerene extract on a Buckyprep column. Conditions: 20 mL injection volume; 10 mL/min toluene flow; 330 nm detecting wavelength.

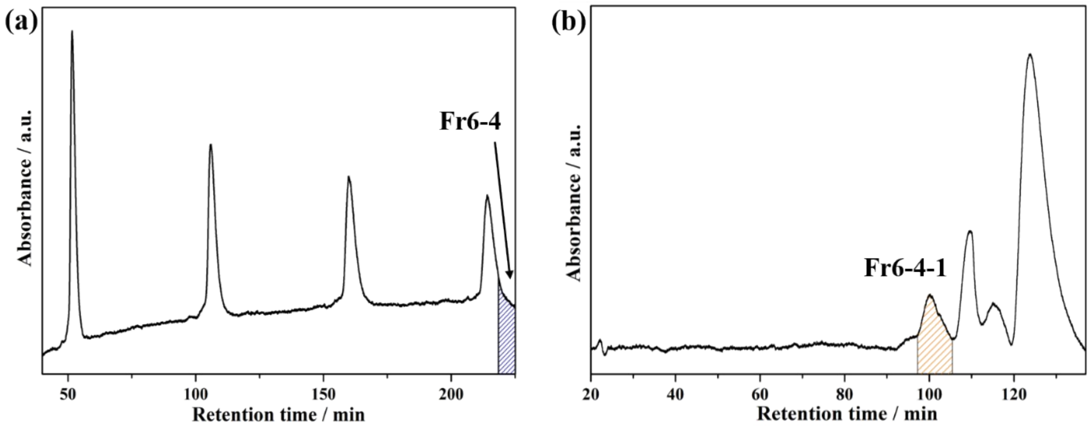

Fig. S2 Isolation schemes of $Lu_3N@C_s(17490)$-C_{76}. (a) Recycling HPLC chromatogram of Fr6 on a Buckyprep column. Conditions: 15 mL injection volume; 10 mL/min toluene flow. (b) HPLC chromatogram of Fr6-4 on a 5PBB column. Conditions: 10 mL injection volume; 10 mL/min toluene flow. (All of the detection wavelengths are 330 nm.)

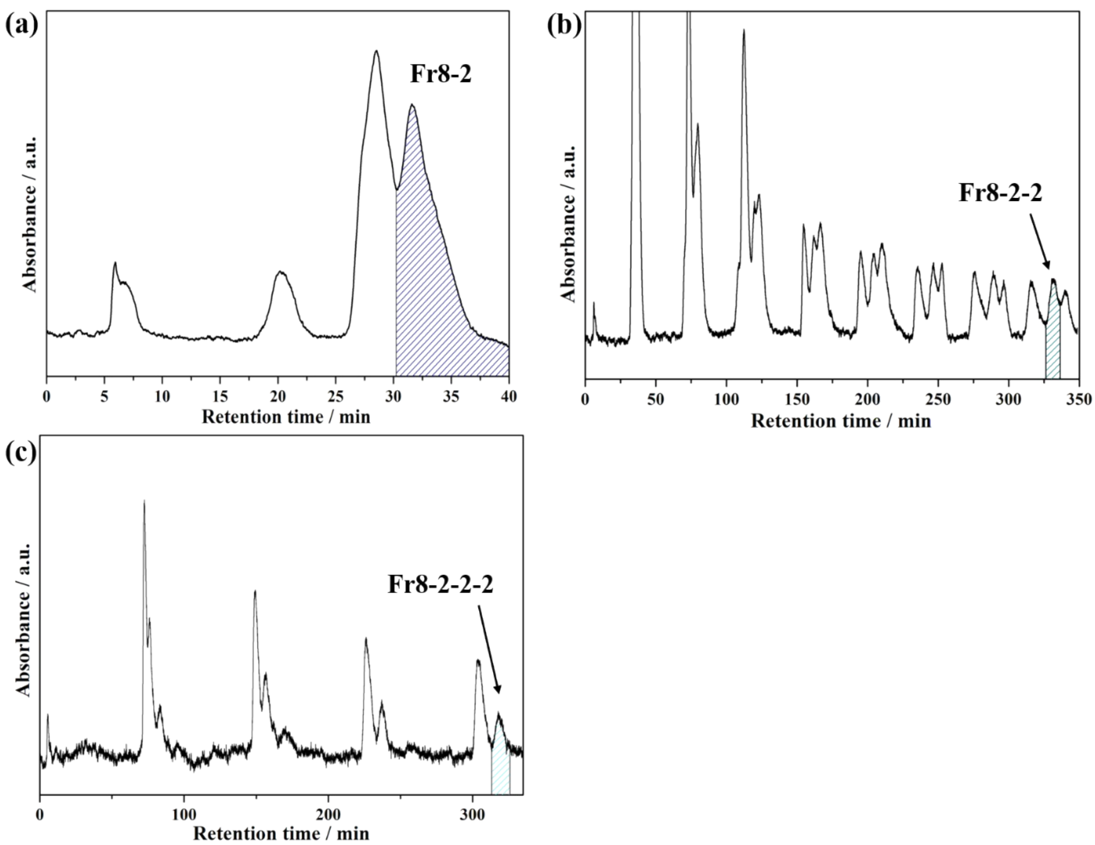

Fig. S3 Isolation schemes of $Lu_3N@C_2(22010)$-C_{78}. (a) HPLC chromatogram of Fr8 on a Buckyprep-M column. Conditions: 20 mL injection volume; 10 mL/min toluene flow. (b) Recycling HPLC chromatogram of Fr8-2 on a Buckyprep-M column. Conditions: 15 mL injection volume; 10 mL/min toluene flow. (c) Recycling HPLC chromatogram of Fr8-2-2 on a Buckyprep column. Conditions: 115 mL injection volume; 10 mL/min toluene flow. (All of the detection wavelengths are 330 nm.)

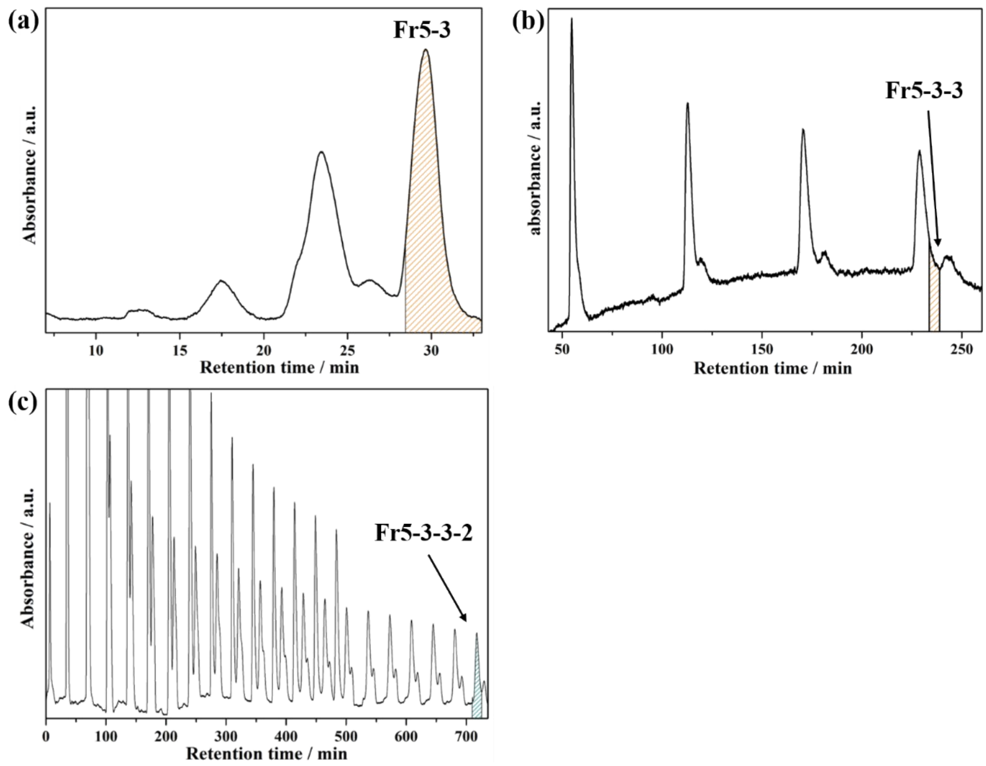

Fig. S4 Isolation schemes of $Lu_3N@D_{3h}(5)$-C_{78}. (a) HPLC chromatogram of Fr5 on a Buckyprep-M column. Conditions: 20 mL injection volume; 10 mL/min toluene flow. (b) Recycling HPLC chromatogram of Fr5-3 on a Buckyprep column. Conditions: 20 mL injection volume; 10 mL/min toluene flow. (c) Recycling HPLC chromatogram of Fr5-3-3 on a Buckyprep column. Conditions: 5 mL injection volume; 4 mL/min toluene flow. (All of the detection wavelengths are 330 nm.)

Table S1. Crystallographic data of $Lu_3N@C_s(17490)$-$C_{76}\cdot Ni^{II}(OEP)$, $Lu_3N@C_2(22010)$-$C_{78}\cdot Ni^{II}(OEP)$, and $Lu_3N@D_{3h}(5)$-$C_{78}\cdot Ni^{II}(OEP)$.

	$Lu_3N@C_s(17490)$-$C_{76}\cdot Ni^{II}(OEP)$	**$Lu_3N@C_2(22010)$-$C_{78}\cdot Ni^{II}(OEP)$**	**$Lu_3N@D_{3h}(5)$-$C_{78}\cdot Ni^{II}(OEP)$**
***T*, K**	100(2)	100(2)	100(2)
***λ*, Å**	0.7336	0.7336	0.7336
color/habit	black/block	black/block	black/block
cryst size, mm	0.14×0.12×0.08	0.25×0.20×0.11	0.04×0.02×0.02
empirical formula	$C_{124}H_{56}Lu_3N_5Ni$	$C_{124}H_{53}Lu_3N_5Ni_{1.04}S_2$	$C_{123}H_{53}Lu_3N_5Ni$
fw	2199.35	2262.45	2184.32
cryst system	monoclinic	monoclinic	monoclinic
space group	*C*2/*m*	*C*2/*m*	*C*2
***a*, Å**	25.1131(5)	26.440(5)	25.3130(3)
***b*, Å**	15.0135(3)	16.808(3)	15.0309(18)
***c*, Å**	19.6714(5)	17.861(4)	19.6730(2)
***α*, deg**	90	90	90
***β*, deg**	93.8870(10)	107.97(3)	95.136(4)
***γ*, deg**	90	90	90
***V*, $Å^3$**	7399.8(3)	7550(3)	7455.0(15)
Z	4	4	4
***ρ*, g/cm^3**	1.974	1.989	1.946
***μ*, mm^{-1}**	4.632	4.611	4.597
R_1 (I > 2\s(I))	0.1197 (7309)	0.0812(6688)	0.1229 (12302)
wR_2 (all data)	0.3260 (8526)	0.2168(7194)	0.3040 (13577)

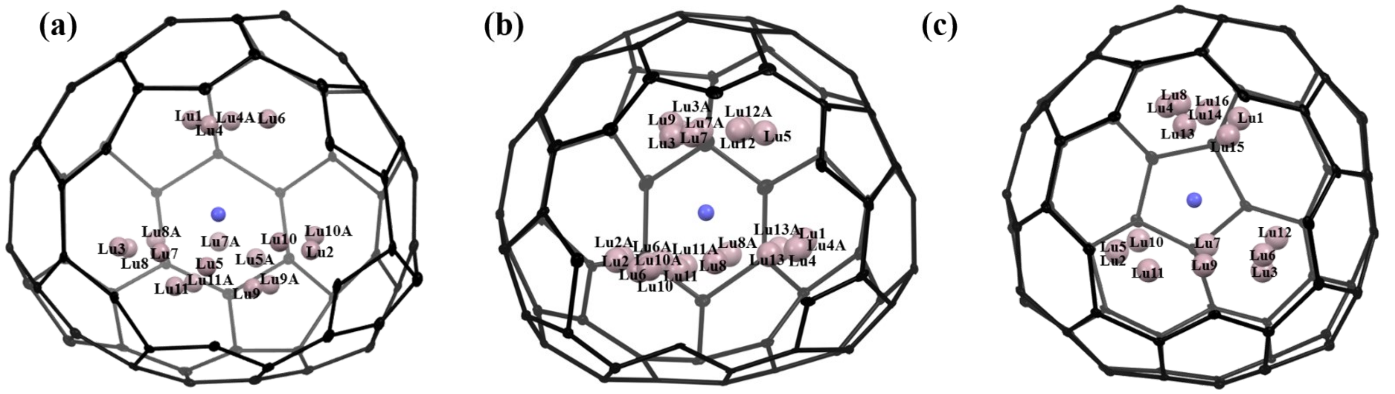

Fig. S5 Positions of the disordered lutetium sites in (a) $Lu_3N@C_s(17490)$-C_{76}, (b) $Lu_3N@C_2(22010)$-C_{78}, and (c) $Lu_3N@D_{3h}(5)$-C_{78} relative to the cage orientation. The Lu sites labeled with “A” are generated by crystallographic operation and a part of the cages are omitted for clarity.

Table S2. The fractional occupancies of the Lu positions in $Lu_3N@C_s(17490)\text{-}C_{76}$, $Lu_3N@C_2(22010)\text{-}C_{78}$, and $Lu_3N@D_{3h}(5)\text{-}C_{78}$.

EMFs	**Fractional occupancy of the Lu positions**						
$Lu_3N@C_s(17490)\text{-}C_{76}$	Lu1/Lu1A	Lu2/Lu2A	Lu3/Lu3A	Lu4/Lu4A	Lu5/Lu5A	Lu6/Lu6A	Lu7
	0.24	0.24	0.11	0.10	0.09	0.06	0.06
	Lu8/Lu8A	Lu9/Lu9A	Lu10/Lu10A	Lu11			
	0.04	0.04	0.02	0.02			
$Lu_3N@C_2(22010)\text{-}C_{78}$	Lu1/Lu1A	Lu2	Lu3/Lu3A	Lu4/Lu4A	Lu5/Lu5A	Lu6/Lu6A	Lu7
	0.22	0.28	0.27	0.26	0.15	0.15	0.12
	Lu8/Lu8A	Lu9/Lu9A	Lu10/Lu10A	Lu11/Lu11	Lu12/Lu12A	Lu13	
	0.06	0.05	0.05	0.04	0.04	0.03	
$Lu_3N@D_{3h}(5)\text{-}C_{78}$	Lu1	Lu2	Lu3	Lu4	Lu5	Lu6	Lu7
	0.36	0.54	0.33	0.37	0.36	0.31	0.13
	Lu8	Lu9	Lu10	Lu11	Lu12	Lu13	Lu14
	0.11	0.11	0.10	0.08	0.06	0.05	0.04
	Lu15	Lu16					
	0.04	0.03					

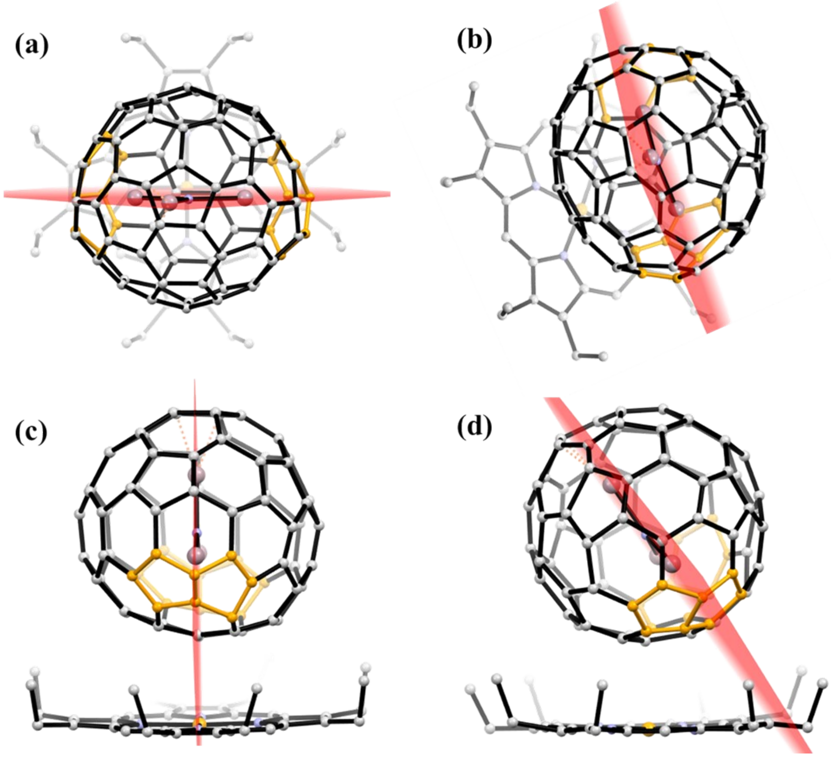

Fig. S6 Relationship of the major Lu_3N sites in (a, c) $Lu_3N@C_s(17490)\text{-}C_{76}$ and (b, d) $Lu_3N@C_2(22010)\text{-}C_{78}$ to the cages and the porphyrins. The Lu_3N planes are marked in red.

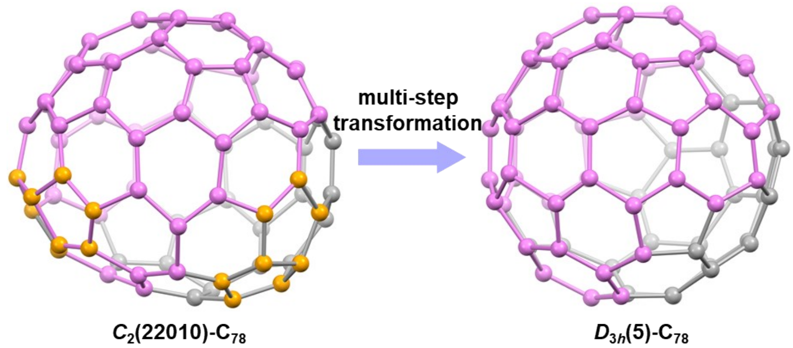

Fig. S7 Structural relationship between C_2(22010)-C_{78} and D_{3h}(5)-C_{78}. The same parts of the two cages are marked in violet. The fused pentagons are highlighted in orange.

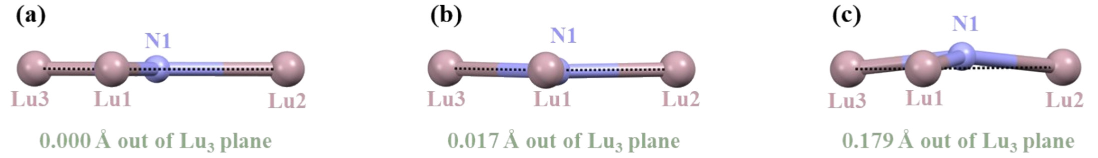

Fig. S8 Drawings showing the planarity of Lu_3N cluster in (a) C_s(17490)-C_{76} and (b) C_2(22010)-C_{78}, and the deviation of the Lu_3N unit from planarity in (c) D_{3h}(5)-C_{78}.